Hierarchical Coordination Scheme for Voltage-Aware Fast Frequency Provision with Flexible Loads

Johanna Vorwerk, Carlo Tajoli, Gabriela Hug
Power Systems Laboratory, ETH Zürich, Zürich, Switzerland
vorwerkj@ethz.ch

***Abstract*—Fast-frequency reserve (FFR) is required to counteract the limited system damping in renewable-rich power systems. Several distributed resources, such as batteries, PVs, and thermal loads, suit this role. However, since the devices are located in distribution grids, local constraints must be considered in the control design. In this work, a coordination scheme is developed to provide FFR without local frequency measurements while using limited communication to the central agent and a neighborhood support system to support local voltages. The proposed scheme is tested through time-domain simulations under diverse grid conditions. The coexistence with other local droop control is evaluated, demonstrating how different types of units with flexible active and reactive power production/consumption can coexist with this scheme. The results highlight that the coordination scheme is a promising alternative to local droop control and can coexist with other schemes.**

***Index Terms*—Distributed Resources, Fast Frequency Control, Hierarchical Coordination, Time-Domain Simulations**

I. Introduction

Replacing synchronous generators with inverter-interfaced renewable generation reduces system inertia and damping while phasing out traditional ancillary service providers [1]. Besides distributed generation and batteries, aggregated thermal loads are a possible resource to procure the required Fast-Frequency Reserve (FFR). However, the design of appropriate controllers that are located in Distribution Networks (DNs) and provide services on Transmission Network (TN) level are still under development [2].

Controlling TN quantities with DN resources poses several challenges. Employing Inverter-Based Generations (IBGs) and Active Thermal Loads (ATLs) located in the DN can lead to voltage and power constraint violations [3]. Employing synchronization devices is required for most local control techniques, as described in [4, 5]. While Phase-Locked Loops (PLLs) are known to significantly impact system stability, particularly single-phase PLLs may destabilize the entire system [6]. In addition, applying these techniques to large aggregations of small thermal loads is costly. In contrast to local schemes, optimization-based schemes ensure reliable operation per se. The literature proposes algorithms that solve a centralized, distributed, or stochastic optimization problem to alternate the power setpoints of the contributing units. Since most real-time implementations require a computation for each control decision, applications are mainly on the time scales of secondary frequency and voltage control [7, 8]. Nonetheless, a few examples of procurement of FFR service exist. For example, [9] suggests a model predictive control algorithm for FFR procurement with IBGs. However, optimal schemes require extensive communication between the control agent and the unit, adding delays and costs. While communication requirements decline for distributed approaches, they are typically studied on a micro-grid scale only. Studies on interactions with neighboring agents are limited. Besides communication, centralized approaches generally face privacy issues as they require either parameters or state information of the local agents.

Some challenges are addressed via hierarchical coordination schemes, such as in [10]. It demonstrates how small-scale IBGs can provide reactive power services to other networks through local commands that change their logic in response to external requests. The local controls operate without knowing the system's or neighborhood's state, but help requests are exchanged with nearby units to foster safe operation.

Inspired by the approach in [10], we derive a coordination scheme for procurement of FFR at TN level through small-scale units in DNs. At the same time, the proposed units monitor the local voltage and power limits and request help from their neighbors if required. The scheme is organized hierarchically: A *central unit* measures the frequency and Rate-of-Change-of-Frequency (ROCOF) and sends a help signal to subordinated *neighborhoods*. Each unit within such a neighborhood responds to the request from the central unit as long as none of its local voltage and power constraints are violated. If the local unit reaches a voltage or power limit, it communicates a help request to its neighbors that, in turn, helps to ensure safe operation. As such, the contributions of the presented work are as follows:

- We develop a coordination scheme suitable for FFR in renewable power systems with small-scale resources. It considers the locality of the resources and supports local grid constraints while providing a service at TN level.
- We demonstrate the effectiveness of the proposed coordination scheme by constructing a large test case and applying the scheme to ATLs and IBGs.
- We assess the scheme's performance when other means of control are active. Indeed, not all units in a system might contribute to the aggregation. Thus, we assess how droop-controlled PV systems affect the response and how the results change when they are integrated into the scheme.

The remainder of the paper mathematically describes the coordination scheme in Section II, discusses the implementation in Section III, outlines the case studies in Section IV and then discusses the implication for a real-world implementation in Section V before concluding the work in Section VI.

II. Proposed Coordination Scheme

This work aims to suggest a hierarchical scheme capable of providing FFR with domestic appliances while maintaining consumer privacy and fostering safe operation. The challenge for such a scheme is to provide a reliable service at the TN

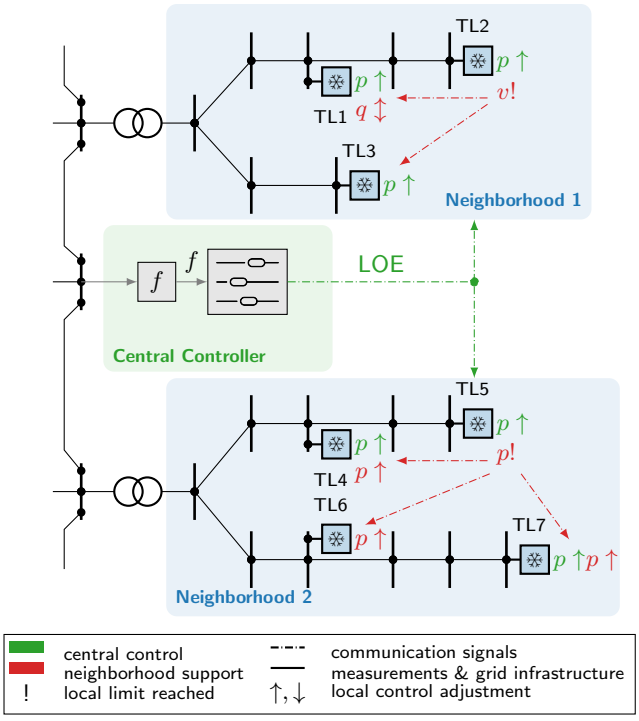

Fig. 1. Overview of the proposed hierarchical control scheme.

level while securing DN constraints. Local control would require reliable local frequency and voltage measurements within each contributing unit but may not meet DN level constraints. On the other hand, central schemes for FFR require fast, hence expensive communication and might request information on the states and margins of contributing units. Furthermore, if unit parameters were required, the service aggregator faces the challenge of collecting and updating this database following seasonal changes and different operating conditions. However, the manufacturers do not specify the parameterization and internal control details of domestic appliances employed in such schemes.

To overcome the mentioned challenges, this work proposes a hierarchical scheme that does not require participants to share private information. While inverter-based thermal loads, called active thermal loads (ATLs), are employed to formulate the scheme, other domestic appliances, such as batteries or IBGs, may be integrated. Since the suggested scheme requires sending signals only in case of a fault, it significantly reduces communication needs.

The suggested scheme contains three modular components communicating through discrete signals: a *central controller*, *local unit-level controls*, and *neighborhood support*. Fig. 1 illustrates the operation of the suggested scheme. Two neighborhoods, each one DN, are connected to the same TN via transformers. At the TN-level, the central controller measures the frequency and, whenever a fault occurs, sends a discrete help request in the form of the Level of Emergency (LOE) to all participating units. This action is represented in green in Fig. 1. The local controllers receive that signal and adjust their active power accordingly if they can. Depending on the severity of the fault, only some units may respond, e.g., in Fig. 1, TL6 does not respond to the request.

The neighborhood support, illustrated with red in Fig. 1, reacts

TABLE I
DEFINITION OF THE LEVEL OF FREQUENCY EMERGENCY ϵ_f AND THE LEVEL OF ROCOF EMERGENCY ϵ_{df}.

Frequency in Hz	ϵ_f	**Rocof in Hz/s**	ϵ_{df}
≤ 48.5	-3	≤ -6.3	-3
$(48.5, 49.5]$	-2	$(-6.3, 2.3]$	-2
$(49.5, 49.9]$	-1	$(-2.3, -0.45]$	-1
$(49.9, 50.1)$	0	$(-0.45, 0.45)$	0
$[50.1, 50.5)$	1	$[0.45, 2.3)$	1
$[50.5, 51.5)$	2	$[2.3, 6.3)$	2
≥ 51.5	3	≥ 6.3	3

when some units cannot meet the demand or a voltage violation is detected. In Neighborhood 1, TL2 notices a voltage violation at its terminal. Thus, it sends a help request to all participating units in the same neighborhood. The electrically close units, such as TL1, adjust their reactive power consumption. At the same time, other units that are further away, such as TL3, do not react. In contrast, TL5 in Neighborhood 2 reaches its active power limit and hence cannot fully meet the demand of the central controller. Instead, it sends a request to all units in the neighborhood, which raises their demand even further. A neighborhood might be defined as one DN, one feeder, or another metric ensuring that the power consumption of one unit affects the terminal voltage of the other units in said neighborhood [10]. In addition, one central unit might be responsible for just one or multiple neighborhoods.

The remainder of this section describes the central controller, the unit-level controls, and neighborhood support.

A. Central Control

The central controller measures the grid frequency, computes a disturbance's severity, and broadcasts a help signal, the LOE, to all contributing units in the areas it is responsible for. It may be positioned at TN-DN-transformers, but also other locations are viable. For regular operation, the LOE equals zero, while it is positive during over-frequencies and negative during under-frequencies. The obtained signal is only sent when it deviates from zero, i.e. during abnormal frequency conditions. Thereby it lowers the communication requirements. During such abnormal conditions, i.e. LOE $\neq 0$, it is sent periodically to adapt the units' support. The LOE depends on estimates of the frequency and the ROCOF. The latter enables fast detection of a disturbance's severity. The central unit computes the ROCOF df as

$$df[k] = T_s^{-1}(f[k] - f[k-1]), \tag{1}$$

where k defines the last available measurement and T_s is the sampling time of the frequency measurement. Note that this technique is applied for demonstration purposes. In an actual implementation, a more robust method should be used.

With the frequency estimate f and the ROCOF measurement, a level of frequency emergency ϵ_f and ROCOF emergency ϵ_{df} are determined by the central unit. The seven bands defined in Table I are used in this work. The appropriate number and width of bands might differ depending on the system. Here, the selected bins are symmetric with a variable width. Preliminary studies were performed to ensure good performance.

The two indicators are merged to obtain one signal for the contributing units. Since the ROCOF is typically large at the instance of a fault, the LOE ϵ is defined differently before and after the frequency deviation reaches its maximum, that is, when

the ROCOF changes its sign for the first time, indicated by the time $t_{\Delta f_{\max}}$. Mathematically, it follows

$$\epsilon[k] = \begin{cases} \text{sgn}(\epsilon_{\text{df}}[k]) \cdot \max\left(|\epsilon_f[k]|, |\epsilon_{\text{df}}[k]|\right), & k \leq t_{\Delta f_{\max}} \\ \epsilon_f[k], & k > t_{\Delta f_{\max}} \end{cases}. \quad (2)$$

Preliminary studies revealed substantial oscillation in the LOE. Thus a 50 mHz deadband between each level of frequency emergency ϵ_f is implemented to achieve a stable signal.

B. Local Controls

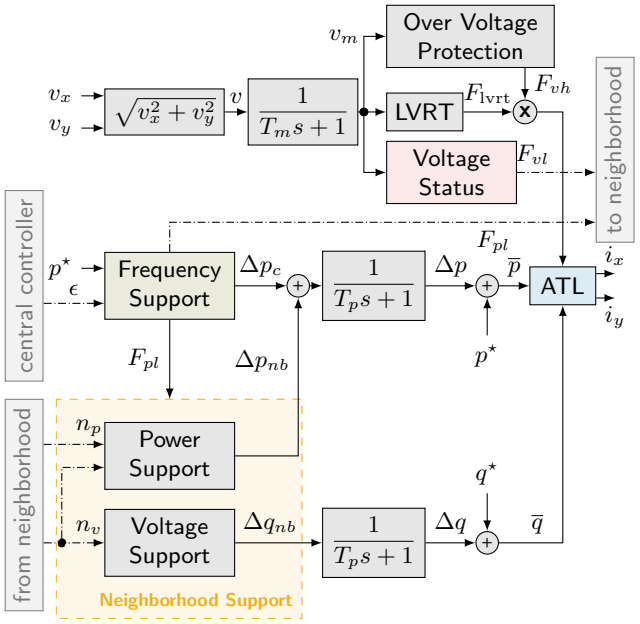

Fig. 2. Overview of the unit-level, local controls for a contributing thermal load.

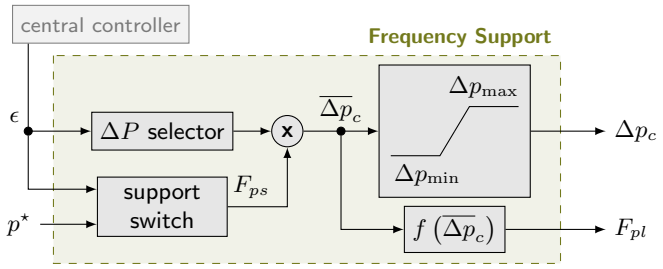

Fig. 3. Local frequency controller and logic for power status updates.

Fig. 2 provides an overview of the implemented unit-level control layer. Note that the ATL model is adjusted from the one derived in [11]. While the overvoltage protection and Low-Voltage-Ride-Through (LVRT) remain in place, the other outer control loops are adjusted to adhere to the hierarchical control scheme. The inner ATL model, the blue block in Fig. 2, is equivalent to the universal thermal load model developed in [12].

The unit receives the LOE signal from the central agent and, considering its power setpoint $p^\star$, decides whether it should react. At the same time, the unit receives voltage and frequency requests from the neighborhood, expressed in terms of n_v and n_p, respectively. Depending on its status and location, the unit might react. The updated power deviations Δp and Δq are passed to the controls of the inner ATL module. Furthermore, the unit checks its limits. When abnormal voltage is detected, the voltage flag F_{vl} is adjusted, and shared with the neighborhood. Similarly, a limit flag on active power F_{pl} is triggered if the unit no longer meets a demand from the central agent.

1) Frequency Support: Fig. 3 depicts the local frequency support logic. It receives the LOE and determines whether to change the active power setpoint based on the pre-disturbance power consumption $p^\star$. The ΔP selector decides how much the power demand should be adapted, whereas the support switch decides if support is provided based on the LOE and the state of the device. The latter sets a flag F_{ps} when the central agent requires frequency support. The computed power change $\overline{\Delta p}_c$ is passed through a limiter that ensures the power setpoint remains within the unit's capabilities. The upper and lower limits, $\Delta p_{\max}$ and $\Delta p_{\min}$, are

$$\Delta p_{\max} = p_{\max} - p^\star, \quad \Delta p_{\min} = -\left(p^\star - p_{\min}\right), \quad (3)$$

where $p_{\max}$ and $p_{\min}$ are the maximum and minimum demand, respectively.

The parallel branch, including $f(\overline{\Delta p}_c)$, detects whether a limit is reached and sets the power limit flag F_{pl} according to

$$F_{pl} = f\left(\overline{\Delta p}_c\right) = \begin{cases} 1, & \overline{\Delta p}_c \geq \Delta p_{\max} \\ -1, & \overline{\Delta p}_c \leq \Delta p_{\min} \\ 0, & \text{otherwise.} \end{cases} \quad (4)$$

The limit flag equals zero in case no limit is reached, is $+1$ when the upper limit and -1 when the lower limit is hit.

For the parameterization of the power selector and support switch, ATL characteristics are considered. While all units provide maximum support during a severe fault (LOE$=\pm 3$), not all should react during low-emergency events. The main priority of ATLs is to keep the controlled temperature within the user-defined bounds. All thermal loads exhibit a direct relationship between the temperature gradient and the power consumption. Thus, a high initial power consumption translates into a significant energy need. If such a unit was required to reduce its consumption for grid support, it would naturally return to a consumption higher than its pre-fault value after the disturbance is cleared. This is called the rebound effect. At the same time, units already operating close to their minimum cannot reduce power consumption much further. Consequently, for low emergency events, it is reasonable to only activate units in the middle of their operating range.

Table II lists the selected parameterization for the power selector and support switch. Generally, the more severe the LOE, the more units react with higher magnitude Δp. This asymmetry is selected to lower the rebound effect. The support switch decides based on the pre-fault operating range p_r that depends on the power setpoint, as well as consumption limits

$$p_r = (p^\star - p_{\min})(p_{\max} - p_{\min})^{-1}. \quad (5)$$

As an example, Table II translates the power ranges to power setpoints for a unit with $p_{\min} = 0.3\,\text{p.u.}$ and $p_{\max} = 1.3\,\text{p.u.}$

2) Voltage Status: The voltage status block detects abnormal voltages at the terminal and sets the voltage limit flag F_{vl}. It is then shared with the neighborhood, which will aim to help. To this end, the two binaries v_{ov} and v_{uv} are switched to one as soon

TABLE II
PARAMETERIZATIONS OF THE UNITS' REACTION.

LOE	-3	-2	-1	0	1	2	3
Δp **[p.u.]**[a]	to $p_{\min}$	-0.3	-0.2	0	0.2	0.3	to $p_{\max}$
p_r **[%]**	all	[15, 75]	[30, 50]	-	[50, 70]	[25, 85]	all
$p^\star$ **[p.u.]**[a,b]	all	[0.45, 1.05]	[0.6, 0.8]	-	[0.8, 1]	[0.55, 1.15]	all

The power change Δp depending on the LOE and the initial operating range p_r. The power range is computed considering the maximum and minimum consumption of a device: $p_r = (p^\star - p_{\min})/(p_{\max} - p_{\min})$.
a The provided power values are in p.u. of the unit's base power.
b Example for a unit with $p_{\min} = 0.3$ p.u. and $p_{\max} = 1.3$ p.u.

as the measured voltage v_m exceeds the upper or lower bound, $v_{\max}$ and $v_{\min}$, i.e.

$$v_{\text{uv}} = \begin{cases} 1, & v_m < v_{\min} \\ 0, & v_m \geq v_{\min}, \end{cases} \quad v_{\text{ov}} = \begin{cases} 1, & v_m > v_{\max} \\ 0, & v_m \leq v_{\max}. \end{cases} \tag{6}$$

If either of the limits is surpassed for more than a lockout time T_{rl}, the voltage limit flag is triggered, and a help request is sent. In mathematical terms, the flag is computed as

$$F_{vl} = \begin{cases} -1, & \int_{t-T_{rl}}^{t} v_{\text{uv}}\, dt \geq T_{rl} \\ 1, & \int_{t-T_{rl}}^{t} v_{\text{ov}}\, dt \geq T_{rl} \\ 0, & \text{otherwise}, \end{cases} \tag{7}$$

such that it is positive for an overvoltage and negative for an undervoltage.

C. Neighborhood Support

Each unit receives the voltage and power limit flags of all other units in its neighborhood. It aims to fulfill the requests based on its own status and closeness to the requesting units.

1) Neighborhood Voltage Support: Units provide voltage support within their neighborhood by adjusting their reactive power, similar to the formulation provided in [10]. As depicted in Fig. 4, the unit receives all voltage limit flags from other devices within its area $\mathcal{H}$. The sum depicts the severity of the situation. The resulting signal n_v is high in magnitude if many units ask for help. It is negative for the occurrence of an undervoltage and positive for an overvoltage event. Since the units should be electrically close to each other and are within one neighborhood, most limit flags should be of the same sign. Considering the number of units requesting help and the reactive power setpoint $q^\star$ the reactive power change $\overline{\Delta q}_{nb}$ is determined as

$$\overline{\Delta q}_{nb} = \begin{cases} n_v q_{\max} \rho_1^v \frac{q_{\max} - q^\star}{(q_{\max} - q_{\min}) + \rho_2^v n_v q_{\max}}, & n_v \geq 0 \\ n_v q_{\max} \rho_1^v \frac{q^\star - q_{\min}}{(q_{\max} - q_{\min}) - \rho_2^v n_v q_{\max}}, & n_v < 0, \end{cases} \tag{8}$$

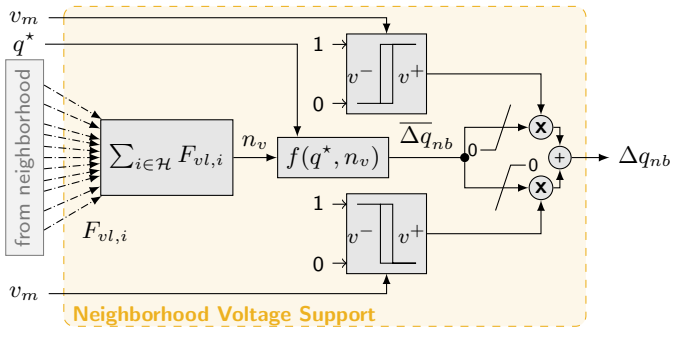

Fig. 4. Reactive power adaptions to support the neighborhood.

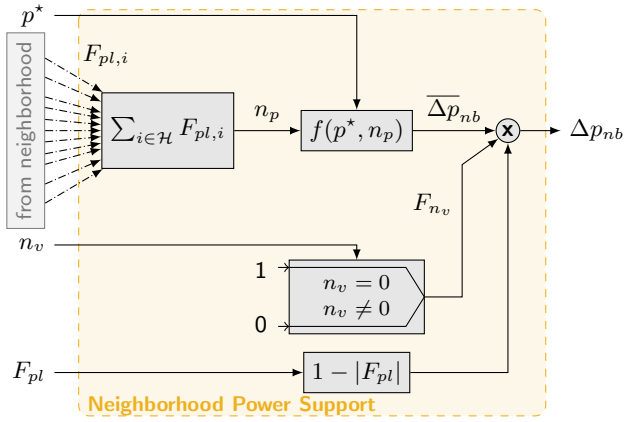

Fig. 5. Active power change to support the neighborhood.

where $q_{\min}$ and $q_{\max}$ denote the unit's lower and upper reactive power limits. Parameters ρ_1^v and ρ_2^v modify the desired reaction. While ρ_1^v is proportional to the reactive power change, ρ_2^v defines how many requests are necessary to dispatch the total available reactive power. Their tuning must account for the size of the neighborhood and the severity of potential voltage violations.

Due to the locality of reactive power, units closer to a voltage violation are more effective in providing support. In addition, the terminal voltages of units close to the area with voltage violations will also be near their limits. Consequently, voltage thresholds are applied such that only the units with a terminal voltage v_m above v^+ will support overvoltages, while only those with a voltage magnitude below v^- help during undervoltages. A hysteresis is applied to prevent continuous switching.

2) Neighborhood Active Power Support: The neighborhood active power support aims to compensate for units that cannot fulfill the central controller's request. Fig. 5 depicts its control logic. All power limit flags from neighboring units are received, summed and the active power adjustment to meet the help requests $\overline{\Delta p}_{nb}$ is obtained by

$$\overline{\Delta p}_{nb} = \begin{cases} n_p p_{\max} \rho_1^p \frac{p_{\max} - p^\star}{(p_{\max} - p_{\min}) + n_p \rho_2^p p_{\max}}, & n_p \geq 0 \\ n_p p_{\max} \rho_1^p \frac{p^\star - p_{\min}}{(p_{\max} - p_{\min}) + n_p \rho_2^p p_{\max}}, & n_p < 0, \end{cases} \tag{9}$$

where $p_{\max}$ and $p_{\min}$ denote the device's maximum and minimum power consumption. The coefficients ρ_1^p and ρ_2^p are used again to achieve the desired response.

This support is only provided when two conditions are met, indicated by the two parallel branches in Fig. 5. The unit will only help if it is not at the power limit itself, i.e., its power limit flag F_{pl} is zero. Furthermore, neighborhood voltage support is prioritized. Hence, the unit only provides active power support to the neighborhood if it receives no voltage help requests and $n_v = 0$ holds. Keeping the voltage within the boundaries is the first goal of the neighborhood, and active power support is allowed only if the voltage remains within bounds.

III. SCHEME IMPLEMENTATION & PARAMETERIZATION

Preliminary simulations to illustrate the scheme's functioning and select the scheme's parameters are conducted on the adjusted CIGRE European 18-bus, residential Low Voltage (LV) network [13]. To achieve a more realistic case, several ATL parameters

TABLE III
FIXED SCHEME AND ATL PARAMETERS.

Coordination Scheme		Active Thermal Loads	
$v_{\max}$	0.2 p.u.	$p_{\max}$	1.3 p.u.
$v_{\min}$	-0.2 p.u.	$p_{\min}$	0.3 p.u.
v_{db}^{+}	0.98 p.u.	$q_{\max}$	0.2 p.u.
v_{db}^{-}	0.94 p.u.	$q_{\min}$	-0.2 p.u.
ρ_1^v, ρ_2^v	0.833, 0.5	$dp_{\max}$	$\pm$ 10 p.u./s
ρ_1^p, ρ_2^p	0.1, 0	$dq_{\max}$	$\pm$ 10 p.u./s
T_{s}	0.05 s	k_p^p	64 p.u.
T_{rl}	1 s	k_i^p	150 p.u./s

are randomly drawn from the uniform distributions defined by the intervals in [11]. Note that the entire modeling of all remaining system components, the initial loading conditions, and the system modifications correspond to the one presented in [11]. This section first details the implementation and parameterization of the proposed coordination scheme. Then, the section illustrates the scheme's functionality through time-domain simulations.

A. Implementation

All simulations are performed using PyRAMSES [14]. A time-domain simulation is conducted as follows: The simulation is interrupted after a fixed sampling time T_s. Then, the central agent shares the LOE with the local units in case of abnormal conditions. The local units may send and receive updated signals to and from the neighborhood. The active and reactive power setpoints are adjusted accordingly. Finally, the simulation is continued with the potentially adjusted setpoints until the next sampling point is reached. The selected sampling time approximates and represents the communication time from the central agent to the local units and within the neighborhood. It is uniform, i.e., in the presented study no additional delays or irregularities are considered.

B. Parameterization

In preliminary studies, the following observations regarding the sampling times arose: high sampling leads to fast reaction and lower ROCOF. The frequency nadir and voltage magnitudes progressively worsened for lower sampling. Yet, for large time steps $> 500\,\mathrm{ms}$, the delayed reaction of the system causes a higher LOE and a stronger reaction from contributing units, highlighting the need to assess the impact of actual communication delays carefully. All remaining studies are conducted with $50\,\mathrm{ms}$ sampling, and future studies should include communication failures, delays, and dropouts.

To select the other parameters, another set of preliminary studies was performed. The final tuning coefficients ρ_1^v and ρ_2^v are set to provide a third of the unit's reactive power in response to a single help request and the full reactive power in case every unit within the neighborhood, that is, six units for the 18-bus system, is requesting it. Consequently, $\rho_1^v = 0.83$ and $\rho_2^v = 0.5$. The voltage help request is sent if the terminal voltage magnitude is outside of its bounds for longer than $T_{rl} = 1\,\mathrm{s}$. All other parameters of the hierarchical scheme are tuned to provide a stable response to a frequency disturbance. Table III summarizes the resulting values of the key parameters.

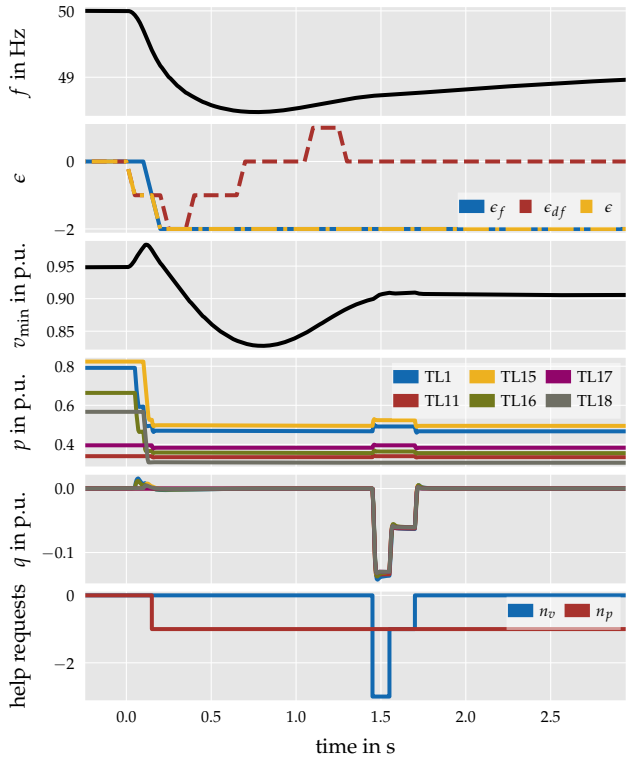

Fig. 6. Exemplary time-domain response to a load step.

C. Exemplary Time-Domain Performance

One set of time-domain simulations is conducted on the 18-bus test case to illustrate and validate the scheme's functionality. The DN represents one neighborhood and is connected to a TN equivalent. The central controller is connected to the High Voltage (HV) side of the transformer. Six ATLs contribute to the hierarchical scheme. The five IBGs generate constant active power, i.e., their frequency droop and voltage control functions are switched off. The system experiences a load step at the HV bus of the transformer at $t = 0\,\mathrm{s}$.

The time-domain response is showcased in Fig. 6. As per definition, the LOE is equal to the minimum of ϵ_f and ϵ_{df} before the frequency nadir is reached. Thereafter, the LOE is $\epsilon = \epsilon_f$. Fig. 6 further displays the ATL terminal active and reactive power, as well as the received power and voltage help requests. TL1 and TL16 change their active power consumption when the LOE reaches -1. Shortly after, at LOE=-2, they increase their support further, and additional units, i.e., TL15 and TL18, react. Since one unit sends a power help request ($n_p = -1$), all other units adjust their active power slightly. TL11 and TL17 only respond to the help request but not to the central controller request due to their initially lower power consumption. Around $t = 1.45\,\mathrm{s}$, the voltage at three buses exceeds the acceptable bounds for longer than the lockout time. Hence, three units send a voltage help request, $n_v = -3$. All ATLs provide help by adjusting their reactive power accordingly until the voltage is restored. Slight adjustments in active power coincide because the units prioritize neighborhood voltage over power support.

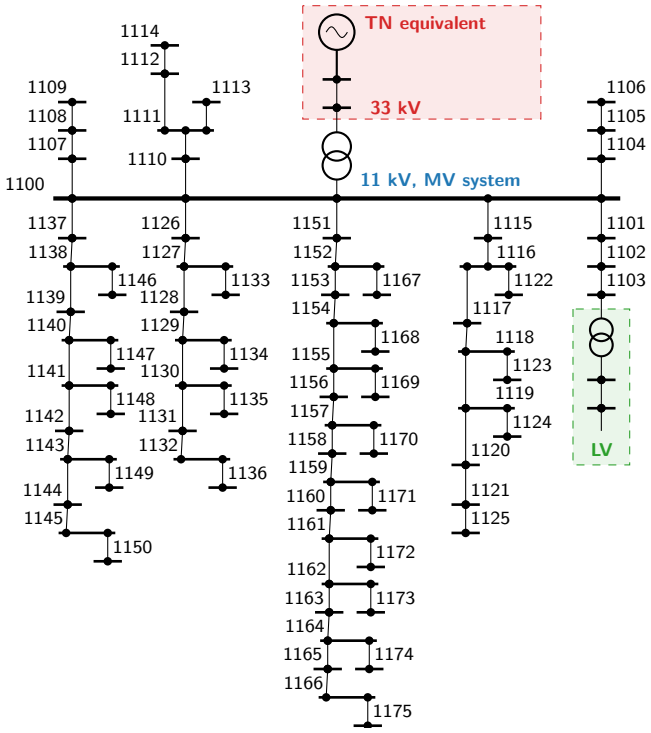

Fig. 7. Adapted 75-Bus test case. Each 11-kV node connects a subordinated 18-bus low voltage (LV) system, as indicated for bus 1103.

IV. Case Study

The hierarchical scheme is tested on an extensive test case with 75 neighborhoods and compared to a classic, local droop control scheme that provides the benchmark for performance assessment. In a real power system, the hierarchical scheme would coexist with other control schemes. Thus, the performed case studies integrate active IBG resources, such as small-scale PV or battery systems. This section first details the test case and outlines five scenarios before depicting the simulation results.

A. Test Case

The 75-bus network from [15] is used to obtain a multi-level test case. While the original Medium Voltage (MV) system only includes the 11-kV voltage level, it is expanded for our case studies. Every MV bus connects one modified 18-bus (LV) system, as used in the preliminary studies and as indicated in Fig. 7. The resulting test case contains 1350 buses, 450 ATLs, and 375 IBGs. Each LV grid is an individual neighborhood, resulting in 75 distinct areas. Note that a single central unit controls all areas, and the scheme's parameterization obtained from tests with one 18-bus system is utilized for this large test case. As in [11], the transmission grid is represented by an equivalent Synchronous Machine (SM) whose parameters are selected to meet the short circuit capacity, inertia constant, and R/X ratio of the TN. The generator's nominal power equals the transformer's. A line is added to adjust the grid strength.

The load and generation present in the original MV system are redistributed to the units in the subordinated LV system. Each LV node consumes a fixed share of the system's load. The same holds for the distributed generation. The load per LV node is randomly redistributed further among the different load types. While ATLs consume 10 % to 30 %, the dynamic share of the background load, modeled by an induction machine, consumes 0 % to 10 % of the LV nodal active power and the remainder is demanded by a static, exponential load model. A uniform distribution applies to draw specific values for each LV node. In contrast, the reactive power is distributed among the static and dynamic components of the background load model only since ATLs operate at unity power factor. Here, the dynamic component consumes 0 % to 10 % of the nodal reactive power demand, while the static component covers the rest. The reader is referred to [11] for details on the models.

B. Scenarios

Five control configurations for ATLs and IBGs are studied:

(i) **Baseline**: ATLs and IBGs do not provide any support. They operate at a constant power factor.
(ii) **Scheme**: ATL and IBGs provide support through the proposed hierarchical scheme.
(iii) **Droop**: ATLs and IBGs are equipped with classic frequency droop control and provide voltage support through their standard control loops.
(iv) **Mixed**: ATLs provide support through the proposed hierarchical scheme, while IBGs use the classic droop control for frequency and their standard voltage support.
(v) **V-help**: ATLs provide support through the proposed hierarchical scheme. The IBGs use their classic droop control for frequency but respond to the voltage help requests through the scheme.

Simulations are conducted for two TN grid equivalents to consider different grid strengths: (i) **Strong**: 6 s inertia, short circuit power of 200 MVA, (ii) **Weak**: 1.5 s inertia, short circuit power of 75 MVA. A load step change is applied at the 33-kV side of the main transformer. Six distinct magnitudes, within ±2 MW, are selected to emulate various over- and under-frequency conditions.

C. Results

Before analyzing the results, note that the droop scheme provides a benchmark to assess the performance of such a hierarchical scheme based on communications against a standard local scheme. Fig. 8 depicts the frequency and minimum voltage trajectories for a 1.5 MW load step in the strong TN. The trajectories suggest that the hierarchical scheme significantly improves and dampens the frequency response. Compared to the baseline, the deviation from the nominal reduces notably. Furthermore, the scheme scenario reduces the ROCOF during the first seconds of the response, as

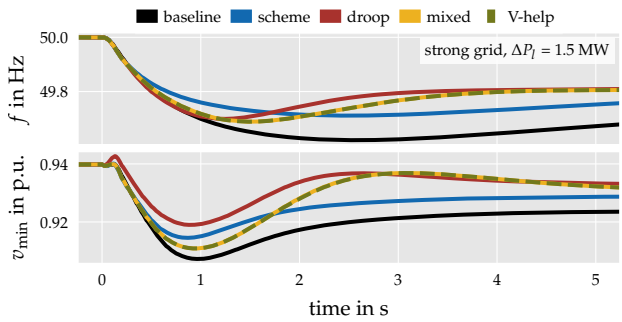

Fig. 8. Exemplary time-domain frequency and minimum voltage response for a strong TN equivalent.

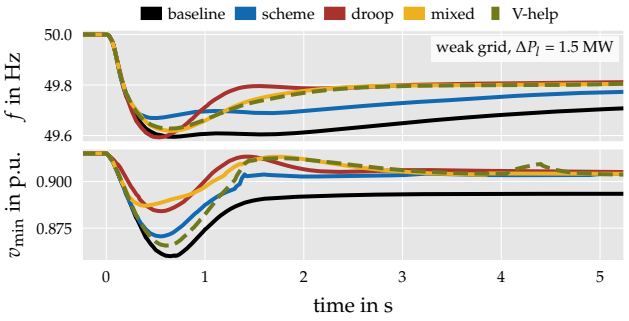

Fig. 9. Exemplary time-domain frequency and minimum voltage response for a weak TN equivalent.

indicated by the slower frequency transient, compared to the droop control scenario. Since the hierarchical scheme uses a ROCOF-based component to estimate the severity, including IBGs in the scheme is better than utilizing droop control. The performances of the hybrid cases, mixed and V-help, overlap for the strong TN. Since the voltage does not violate any threshold, no support is activated. Their frequency performances are similar to the droop response. Compared to the baseline, the response speeds up while the frequency deviation is reduced.

The situation differs for the weak TN, as presented in Fig. 9. Here, the scheme clearly provides the best frequency performance regarding the maximum frequency deviation, followed by the hybrid and the droop scenarios. The latter has a frequency nadir comparable to the baseline. Regarding the voltage magnitude, the droop control achieves the best responses. The mixed case behaves similarly to the droop, while V-help exhibits the lowest voltage magnitude for any scenario employing control.

The absolute of the maximum frequency deviation for all six load steps is depicted in Fig. 10. The frequency deviation is almost always the lowest for the strong and weak grids when all units are fully incorporated into the scheme. This holds especially for the weak TN. In the case of a weak TN, droop control performs similarly to the baseline, and the hybrid schemes are superior.

Fig. 11 summarizes the maximum voltage magnitudes for the over-frequency and the minimum voltage magnitudes for the under-frequency events. It supports the previous findings: The results suggest a required trade-off between frequency and voltage. Droop control generally results in the best voltage performance. In the case of a weak system, the mixed scenario appears more effective in increasing minimum voltages than the V-help strategy. This finding highlights a potential need to retune the voltage support mechanism for the large test case. The results indicate superior performance when IBGs operate with the voltage control loops defined in [11].

V. Implications for Real-World Implementations

The simulations suggest that the proposed scheme offers an effective alternative to local droop control. This section discusses required adjustments and considerations before applying the scheme to real-world power systems.

First and foremost, the scheme's efficacy highly depends on its parameterization and the TN strength. The presented studies should be revised and repeated for the respective power system. This especially holds for the parameterization of the neighborhood support. For the selected strong grid, the proposed hierarchical

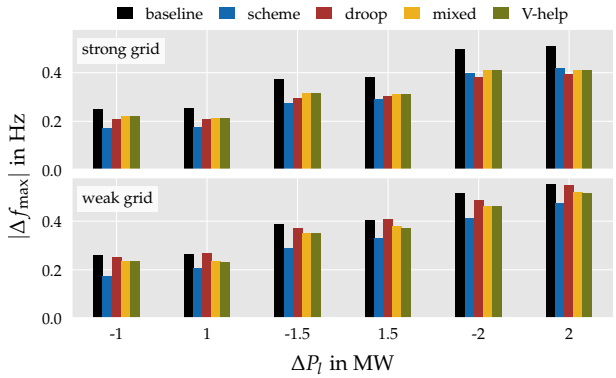

Fig. 10. Absolute maximum frequency deviation $|\Delta f_{\max}|$ during different load steps Δp_L per IBG support option.

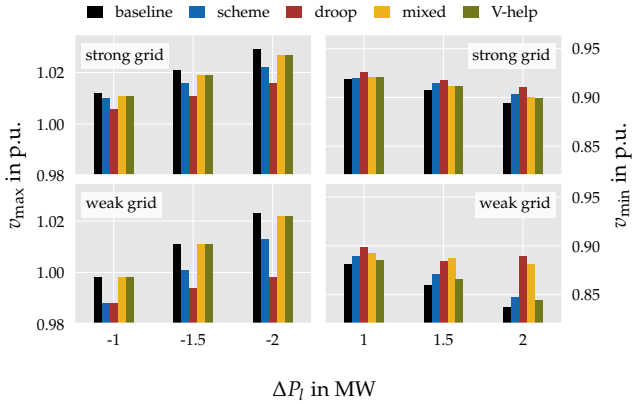

Fig. 11. Critical voltage during different load steps Δp_L per IBG support option.

control has a limited impact on the system's frequency and voltage. The significant differences between the scheme and droop options suggest that using the tuned parameters from the small test case is suboptimal. Furthermore, voltage-dependent background loads influence the scheme's effectiveness. Specific adjustments for each system and experience with its operation are necessary. Ideally, a real-world implementation will permit remote access to adjust the required parameters of the hierarchical control scheme.

In addition, the scheme employs devices that are typically interfaced via single-phase connections at the lowest voltage levels. However, the presented study considered balanced, three-phase MV and LV networks. With single-phase connections, the impact of the voltage help provided by units connected to one phase supporting those on another phase might be limited. Even so, if the selected neighborhoods are large enough and contain sufficient devices in each phase, the scheme could still provide a promising alternative. Nonetheless, additional studies should be conducted to define the ideal size of a neighborhood when considering the single-phase unbalanced nature of LV networks.

The suggested scheme could be improved further by redefining the reaction for a given emergency and the different LOE levels. In particular, the power ranges that define the units that are activated for each level of emergency could consider the inherent temperature dynamics of thermal loads and the capabilities of a heterogeneous aggregation. Temperature dynamics and consumer comfort have not been considered in this work due to the small time scales of the simulations. Indeed, [16] has shown that temperatures and, hence, consumer comfort are only slightly impacted

on FFR operation time scales. However, temperature dynamics are essential when identifying the scheme's efficacy for daily, seasonal, and annual consumption patterns.

A detailed study of the bus voltage sensitivity to the change in active and reactive power of the ATLs could provide insights into the neighborhood concept and possibly improve the scheme's performance. Considering the coupling of active power and voltage, which is more prevalent in DNs, might significantly enhance the support for DN reserve provision. In addition, only one location for the central agent was tested. Depending on the overall control goals, the position of the central agent within a larger TN system is crucial, especially for weaker or larger systems that are subject to local frequency deviations [17, 18]. Considering that local FFR helps improve the frequency the most, weak systems might benefit from using multiple dispersed central agents.

Finally, investigating suitable communication systems, their capabilities, and their costs permits an in-depth understanding of the potential and limitations of technical and economic aspects. The neighborhoods of the proposed scheme operate independently. In case of a single communication failure, e.g., a signal is delayed, not received, or sent by a contributing unit, only the neighborhood the failure occurred in is affected. Furthermore, the contribution of each individual unit to the entire control reaction is negligible. Thus, communication failures or delays should have a minor impact if most contributing units receive the signal of the central agent. As such, the entire hierarchical approach is resilient against single-point communication failures. Nonetheless, the performed study of communication times, delays, and sampling should be extended when implementing it in an actual power system.

VI. Conclusions & Outlook

This paper introduces a coordination scheme that does not require local frequency measurements. Instead, a central agent estimates a disturbance's severity by evaluating the frequency and the ROCOF. It shares the LOE with participating units that adjust their power consumption. In addition, predefined neighborhoods support local voltages. The units within one area request help when they detect a voltage violation at their terminals. Similarly, units may request additional support within the same area when they cannot meet the central agent's request. This design keeps communication at a minimum. As such, the presented scheme is a cost-effective alternative to centralized and local control schemes.

The scheme is first tested on a small 18-bus network to demonstrate its operation and perform a parameter study. Once the final parameters are obtained, the scheme is tested on a large-scale MV system, including 75 individual neighborhoods. Several control configurations regarding the integration of IBGs and coexistence with local droop control are studied. The proposed scheme shows promising results in enhancing the frequency deviation and preventing the activation of voltage protection. Generally, performance is best when many devices are fully incorporated into the scheme. Since IBGs reserve is larger for the considered test case, integrating them in the scheme is particularly effective. In this case, the scheme is more effective than droop control due to the ROCOF-based estimation of the situation's severity. This achievement arrives with a cost of poorer performance in terms of voltage. In contrast, lower voltages enhance the self-regulating effect of voltage-dependent loads, and thus frequency is further improved. Systems prone to voltage problems may benefit from integrating as many devices as possible in the neighborhood voltage support. Future research should investigate the scheme's robustness against communication delays and malfunction as well as the effective parameterization of the scheme in the context of bulk power systems with multiple central control units.

References

[1] F. Milano, F. Dörfler, G. Hug, D. J. Hill, and G. Verbič, "Foundations and challenges of low-inertia systems," in *PSCC*, Dublin, 2018.

[2] S. Chatzivasileiadis, P. Aristidou, I. Dassios, T. Dragicevic, D. Gebbran, F. Milano, C. Rahmann, and D. Ramasubramanian, "Micro-flexibility: Challenges for power system modelling and control," in *2022 Power Systems Computation Conference (PSCC), Porto*, 2022.

[3] S. C. Ross, G. Vuylsteke, and J. L. Mathieu, "Effects of load-based frequency regulation on distribution network operation," *IEEE Trans. Power Syst.*, vol. 34, pp. 1569–1578, 3 2019.

[4] U. Markovic, "Towards reliable operation of converter-dominated power systems: Dynamics, optimization and control," Doctoral Thesis, ETH Zurich, Zurich, 2020.

[5] H. Karbouj, Z. H. Rather, D. Flynn, and H. W. Qazi, "Non-synchronous fast frequency reserves in renewable energy integrated power systems: A critical review," *Int. J. Electr. Power Energy Syst.*, vol. 106, pp. 488 – 501, 2019.

[6] J. Xu, H. Qian, Y. Hu, S. Bian, and S. Xie, "Overview of sogi-based single-phase phase-locked loops for grid synchronization under complex grid conditions," *IEEE Access*, vol. 9, pp. 39 275–39 291, 2021.

[7] M. Almassalkhi, S. Brahma, N. Nazir, H. Ossareh, P. Racherla, S. Kundu, S. P. Nandanoori, T. Ramachandran, A. Singhal, D. Gayme, C. Ji, E. Mallada, Y. Shen, P. You, and D. Anand, "Hierarchical, Grid-Aware, and Economically Optimal Coordination of Distributed Energy Resources in Realistic Distribution Systems," *Energies*, vol. 13, no. 23, p. 6399, 2020.

[8] M. A. I. Khan, S. Paudyal, and M. Almassalkhi, "Performance Evaluation of Network-Admissible Demand Dispatch in Multi-Phase Distribution Grids," in *11th Bulk Power Systems Dynamics and Control Symposium*, Banff, 2022.

[9] O. Stanojev, U. Markovic, P. Aristidou, G. Hug, D. Callaway, and E. Vrettos, "Mpc-based fast frequency control of voltage source converters in low-inertia power systems," *IEEE Trans. Power Syst.*, vol. 37, no. 4, pp. 3209–3220, 2022.

[10] G. Valverde, D. Shchetinin, and G. Hug-Glanzmann, "Coordination of distributed reactive power sources for voltage support of transmission networks," *IEEE Trans. Sustainable Energy*, vol. 10, pp. 1544–1553, 7 2019.

[11] J. Vorwerk, U. Markovic, P. Aristidou, and G. Hug, "Quantifying the uncertainty imposed by inaccurate modeling of active distribution grids," in *2022 Power Systems Computation Conference (PSCC), Porto*, 2022.

[12] J. Vorwerk, U. Markovic, and G. Hug, "Fast demand response with variable speed thermal loads - towards universal modeling for stability assessment," in *2021 North American Power Symposium (NAPS)*, 2021.

[13] *Benchmark systems for network integration of renewable and distributed energy resources*. CIGRE, 2014.

[14] P. Aristidou, S. Lebeau, and T. V. Cutsem, "Power system dynamic simulations using a parallel two-level schur-complement decomposition," *IEEE Trans. Power Sys.*, vol. 31, no. 5, pp. 3984–3995, 09 2016.

[15] G. Chaspierre, "Reduced-order modelling of active distribution networks for large-disturbance simulations," Ph.D. dissertation, Universite de Liege, Belgium, 2020.

[16] J. Vorwerk, U. Markovic, P. Aristidou, E. Vrettos, and G. Hug, "Modelling of variable-speed refrigeration for fast-frequency control in low-inertia systems," *IET Smart Grid*, vol. 3, no. 6, pp. 924–936, 2020. [Online]. Available: https://ietresearch.onlinelibrary.wiley.com/doi/abs/10.1049/iet-stg.2020.0154

[17] AEMO, "Fast frequency response implementation options," 2021.

[18] G. Misyris, D. Ramasubramanian, P. Mitra, and V. Singhvi, "Locational aspect of fast frequency reserves in low-inertia systems – control performance analysis," in *11th Bulk Power Systems Dynamics and Control Symposium*, Banff, 2022.